

## Anomalously slow domain growth due to a modulus inhomogeneity in phase-separating alloys

Akira Onuki and Hiraku Nishimori

*Yukawa Institute for Theoretical Physics, Kyoto University, Kyoto 606, Japan*

(Received 9 January 1991)

We simulate spinodal decomposition in alloys when the two phases have different shear moduli. In late stages, softer regions are anisotropically deformed and harder regions tend to be isotropic. This leads to morphologies with very slow coarsening rates. We find glassy states in which softer regions form a percolated network wrapping isotropic harder regions.

It is widely recognized that the domain morphology in phase-separating alloys can be radically influenced by elastic fields originating from the lattice misfit or the difference in the lattice constants of the two phases.<sup>1</sup> In particular, elastic anisotropy of crystals and/or anisotropy brought about by external stresses gives rise to modulated structures with nearly periodic patterns in late-stage spinodal decomposition. As regards the growth of modulated structures, Carpenter<sup>2</sup> observed that the time exponent  $a$  for the domain size in Au-Pt alloys strongly depends on the composition:  $1/a = 4.8, 9.3,$  and  $3.2,$  respectively, for 40:60, 60:40, 80:20 Au-Pt alloys. More strikingly, in alloys with relatively large lattice misfits, Miyazaki *et al.*<sup>3</sup> found that the coarsening rate becomes extremely slow and the domain growth virtually stops near the critical composition. Although these observations have not yet been adequately explained, their origin should undoubtedly be ascribed to the elastic effects.<sup>3</sup>

A Ginzburg-Landau approach has recently been presented to analyze the elastic effects in phase-separating alloys.<sup>4</sup> We assume the coherent condition, which states that the lattice planes are continuous through the interfaces.<sup>5</sup> We obtain a closed description of the composition  $c$  only by eliminating the elastic field from mechanical equilibrium. There arise three elastic contributions to the effective free energy: (i) a long-range interaction due to the cubic anisotropy, (ii) a dipolar one due to external stresses, and (iii) a long-range one due to elastic modulus difference between the two phases. The first two interactions are bilinear in  $c$ , while the third is cubic in  $c$ . Then we have performed a computer simulation<sup>6</sup> in two dimensions by taking into account the first two long-range interactions. It has resulted in a tweed pattern due to cubic elasticity, a lamellar pattern under a uniaxial stress along the [10] direction, and a unique oblique pattern under a shear stress. In all these cases, domains are rectangular stripes with their longer sides perpendicular to the softest directions. They have continued to grow up to the system size obeying the growth law  $a \equiv \partial[\ln R_{11}(t)]/\partial[\ln t] \sim 0.2$  at the critical composition, where  $R_{11}(t)$  is the characteristic size in the [11] direction. This value of 0.2 is considerably smaller than the usual value  $\frac{1}{3}$  which results from the model without elasticity.<sup>7</sup> The slower coarsening in our case originates from the fact that the interface motion in lamellar-like regions is much slower than near the ends of long stripes.

The aim of this paper is to study the effects of the modulus difference between the two phases or,

equivalently, the role of the third long-range interaction mentioned above in our scheme. To examine this aspect most unambiguously, we assume isotropic elasticity without external stresses. Then, the first two interactions treated previously are now nonexistent. However, the shear modulus  $\mu$  depends weakly on the composition  $c$  as<sup>4</sup>

$$\mu = \mu_0 + \mu_1 c, \quad (1)$$

while the bulk modulus is a constant  $K_0$  independent of  $c$ . Here  $c$  is a conserved order parameter measured from the critical value for the coherent free energy (see below). It is coupled with the elastic field  $\mathbf{u}$  in the free energy as

$$F = \int d\mathbf{r} [ f_0(c) + \frac{1}{2}(\nabla c)^2 + \alpha c \nabla \cdot \mathbf{u} + \frac{1}{2} K_0 (\nabla \cdot \mathbf{u})^2 + (\mu_0 + \mu_1 c) Q ], \quad (2)$$

where  $f_0$  is a Ginzburg-Landau free-energy density and  $\alpha$  is the coupling constant. The  $\mathbf{u}$  is the displacement vector from some homogeneous reference state. The  $Q$  arises from anisotropic deformations,

$$Q = \frac{1}{4} \sum_{i,j} \left[ \nabla_i u_j + \nabla_j u_i - \delta_{ij} \frac{2}{d} \nabla \cdot \mathbf{u} \right]^2, \quad (3)$$

where  $\nabla_i \equiv \partial/\partial x_i$  and  $d$  is the spatial dimensionality.

We eliminate  $\mathbf{u}$  from the mechanical equilibrium condition  $\delta F/\delta u_i = 0$ . When  $\mu_1 = 0$ , this task can be readily performed to give Cahn's coherent free-energy density,<sup>8</sup>  $f(c)$ , which differs from  $f_0(c)$  in (2) by a term proportional to  $c^2$ . The elastic field induced by inhomogeneities of  $c$  is given by  $\delta u_i = -(\alpha/K_{L0})\partial w/\partial x_i$ , where  $K_{L0} = K_0 + 2(1 - 1/d)\mu_0$  and  $w$  is determined by

$$\nabla^2 w = c - \bar{c}, \quad (4)$$

$\bar{c}$  being the average order parameter. When  $|\mu_1 c|$  is much smaller than  $\mu_0$  for any typical values of  $c$ , we may treat  $\mu_1$  as a small expansion parameter to obtain an effective free energy for  $c$  to first order in  $\mu_1$ ,

$$F = \int d\mathbf{r} [ f(c) + \frac{1}{2}(\nabla c)^2 + \mu_1 (\alpha/K_{L0})^2 c \hat{Q} ] \quad (5)$$

with

$$\hat{Q} = \sum_{i,j} \left[ \nabla_i \nabla_j w - \frac{1}{d} \delta_{ij} \nabla^2 w \right]^2. \quad (6)$$

The last term in (5) turns out to be a very intriguing

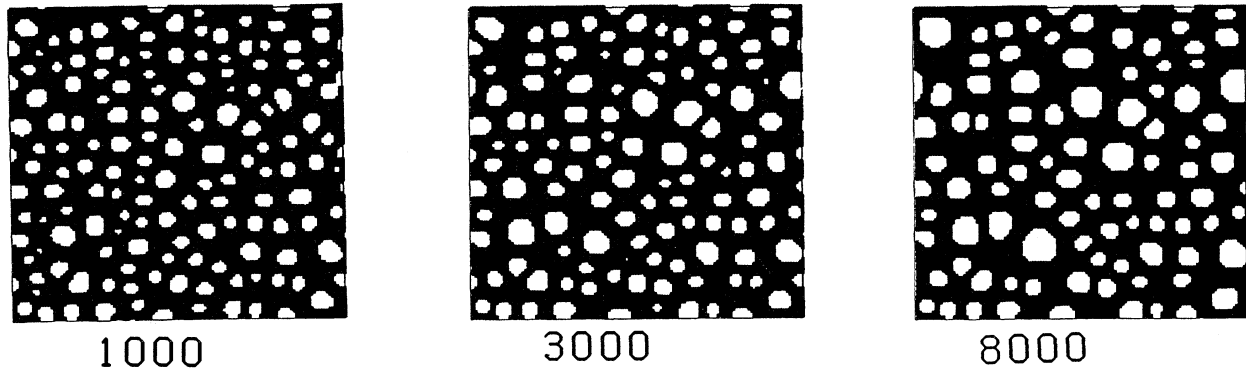


FIG. 1. Evolution patterns at  $\phi_s = 70\%$  and  $g_E = 0.07$ . The numbers below the figures are the times after quenching. The time step is taken to be unity.

long-range interaction. We already showed<sup>4</sup> that it causes a shape bifurcation of an isolated softer domain from spheres into plates as predicted by Johnson and Cahn<sup>9</sup> and that it gives rise to a pairwise interaction between separate domains (see the last part of this paper).<sup>10</sup>

Hereafter, we focus our attention on the role of the last term in spinodal decomposition by assuming the form  $f = -\frac{1}{2}\tau c^2 + \frac{1}{4}c^4$  with  $\tau > 0$  (in the unstable region). Then the compositions and the shear moduli in the two phases are different by  $\Delta c = 2\tau^{1/2}$  and  $\Delta\mu = \mu_1 \Delta c$ . Notice that the last term in (5) is positive in harder regions (where  $\mu_1 c > 0$ ) and negative in softer regions (where  $\mu_1 c < 0$ ). It is minimized in morphologies in which harder domains assume spherical shapes and softer domains are, instead, anisotropically deformed, if interactions among domains are neglected. Such asymmetric shape changes can lower the free energy by  $(\Delta\mu)\epsilon^2 R^3$  per typical domain, where  $\epsilon [\sim (\alpha/K_{L0})\Delta c]$  is a typical strain and  $R$  is the domain size. On the other hand, the surface free energy is  $\sigma R^2$ ,  $\sigma$  being the surface tension. Equating these two free-energy contributions, we find a crossover radius given by

$$R_E \sim \sigma / (\Delta\mu)\epsilon^2. \quad (7)$$

For  $R > R_E$ , softer domains tend to be deformed into plates if their volume fraction  $\phi_s$  is small. If  $\phi_s$  is not small, they will be percolated to form a network. Here we assume  $R_E \gg \xi (\sim \tau^{-1/2})$ , where  $\xi$  is the interfacial thickness or the thermal correlation length. This regime is called the weakly inhomogeneous case. However, notice that  $R_E$  does not depend on  $\tau$  ( $\propto T_c - T$ ) from  $\sigma \sim \tau^{3/2}$  and  $\Delta\mu \sim \epsilon \sim \tau^{1/2}$  near criticality in mean-field theory. Then we may well expect the existence of the strongly inhomogeneous case  $R_E \lesssim \xi$  near criticality. The study of this anomalous regime will be deferred to a forthcoming paper.

We numerically solve the following diffusion-type equation in two dimensions:

$$\begin{aligned} \frac{\partial}{\partial t} c = \nabla^2 (\delta F / \delta c) = \nabla^2 [(-1 - \nabla^2 + c^2)c + g_E \hat{Q}] \\ + 2g_E \sum_{i,j} \nabla_i \nabla_j c [\nabla_i \nabla_j w - \frac{1}{2} \delta_{ij} (c - \bar{c})]. \end{aligned} \quad (8)$$

Here we have set  $\tau = 1$  in  $f$ , and  $w$  and  $\hat{Q}$  are defined by (4) and (6). The parameter  $g_E \equiv \mu_1 (\alpha/K_{L0})^2 \tau^{-1/2}$

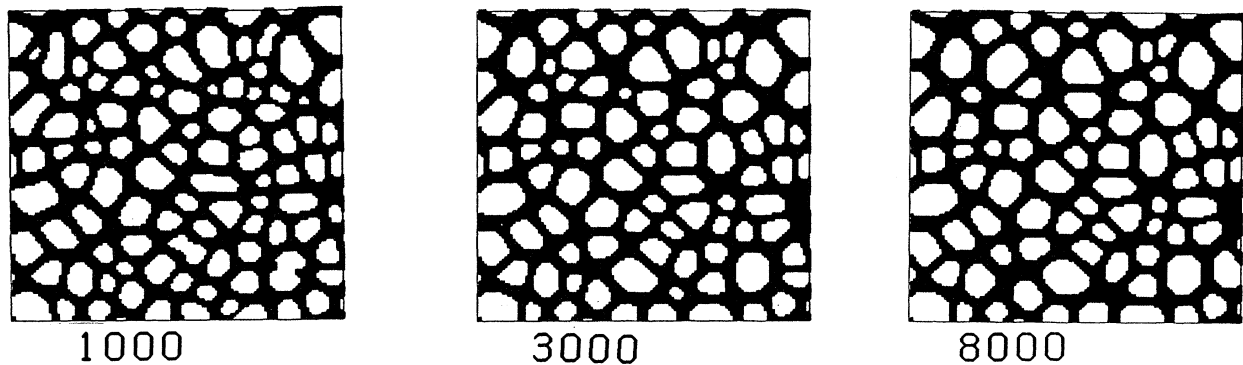


FIG. 2. Evolution patterns at  $\phi_s = 50\%$  and  $g_E = 0.07$ .

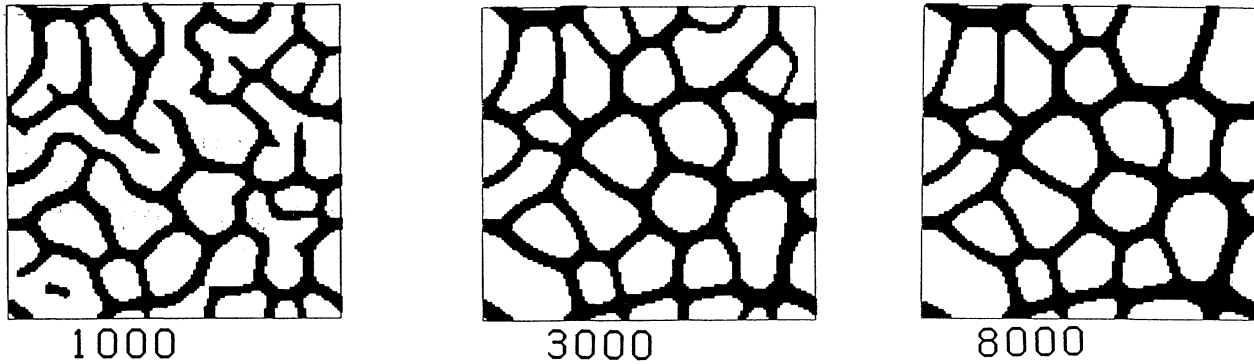


FIG. 3. Evolution patterns at  $\phi_s = 30\%$  and  $g_E = 0.07$ .

represents the strength of the modulus inhomogeneity being of order  $\xi/R_E$  and is assumed to be much smaller than 1.

We use Oono and Puri's method<sup>7</sup> to investigate (8) as in Ref. 6. The system is a  $128 \times 128$  square lattice with the periodic boundary condition and is quenched at  $t = 0$  from a disordered configuration. Our strategy to calculate  $w$ , (4), is to integrate the diffusion equation  $\partial\mu/\partial t' = \frac{1}{2}(\nabla^2\mu - c_n(\mathbf{r}) + \bar{c})$  from  $t' = 0$  to 20 at each mapping, where  $c_n(\mathbf{r})$  is the concentration field at  $t = n$  held fixed in this  $t'$  integration. We write the resultant solution as  $\mu_n(\mathbf{r})$ . At long wavelengths, its Fourier transform satisfies  $\mu_n(\mathbf{k}) = \zeta_k \mu_{n-1}(\mathbf{k}) - (1 - \zeta_k) k^{-2} c_n(\mathbf{k})$ , where  $\zeta_k = \exp(-10k^2)$ . Notice that  $\mu_{n-1}(\mathbf{r})$  obtained at the previous step is used as the initial value of  $\mu$  in the  $t'$  integration at  $t = n$ . Here we simply set  $\mu_n(\mathbf{r})$  equal to

$w_n(\mathbf{r}) \equiv \nabla^{-2}[c_n(\mathbf{r}) - \bar{c}]$ , neglecting nonvanishing  $\zeta_k$ , and perform an Oono-Puri mapping to obtain  $c_{n+1}(\mathbf{r})$ . Because  $c_n$  changes very slowly for large  $n$ ,  $\mu_n$  should relax to  $w_n$  for large  $n$  even at long wavelengths, for which  $\zeta_k \approx 1$ . In fact, the differences between  $\nabla^2\mu_n$  and  $c_n - \bar{c}$  have been confirmed to be very small ( $\lesssim 10^{-4}$ ) for large  $n$  ( $\gtrsim 10^3$ ) except for the interfacial regions.

We have found that the domain growth is dramatically slowed down in the presence of the new terms ( $\sim g_E$ ) in (8). In fact, we have obtained  $a \approx \frac{1}{3}$  by setting  $g_E = 0$  with the other conditions kept unchanged. Figures 1–3 show the results for  $g_E = 0.07$ . The numbers below the figures are the times after quenching. The solid regions represent the softer domains with  $g_E c < 0$ , while the open regions represent the harder domains with  $g_E c > 0$ . The volume fraction  $\phi_s$  of the softer component is 70, 50, and 30% in Figs. 1–3, respectively. Figure 4 displays the perimeter length of the interface regions for  $g_E = 0.07$  and 0.05, where the curves are averages of four runs. It is expected to be inversely proportional to the domain size and its slope is defined as  $-a$ . At  $\phi_s = 70\%$   $a$  is about 0.12 for  $t \gtrsim 200$ . For  $\phi_s = 50\%$  and 30%, the coarsening almost stops and we find  $a \lesssim 0.04$  after a certain crossover time  $t_E$ , where the softer component forms a percolated network structure enclosing the harder domains. Let  $a_0$  be the time exponent for  $t \lesssim t_E$ . Then we expect

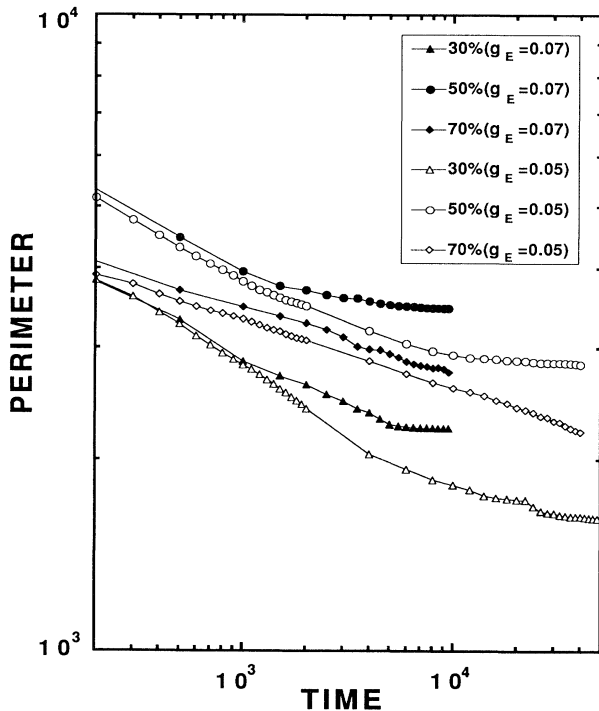


FIG. 4. Perimeter length vs. time. The mesh size and time step are unity.

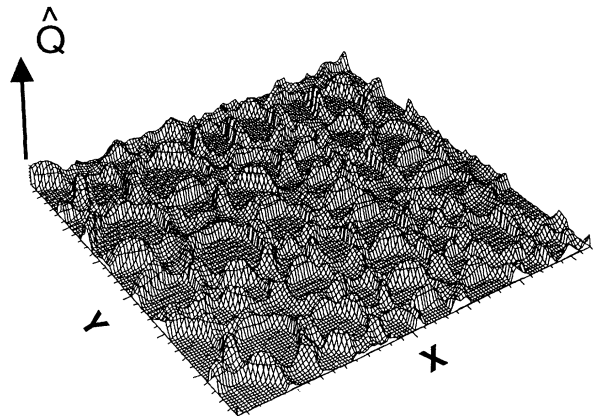


FIG. 5. The degree of anisotropic deformations  $\hat{Q}$  at  $t = 45000$  for  $g_E = 0.05$ .

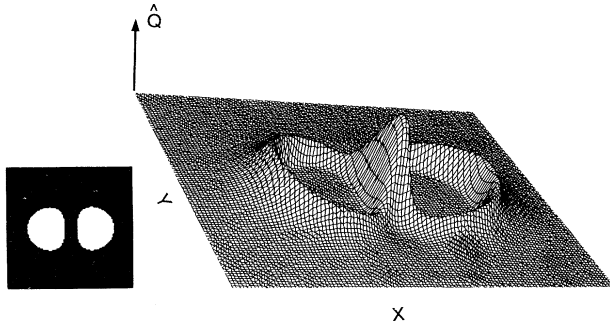


FIG. 6. Shape changes of two harder domains at  $t = 1000$  for  $g_E = 0.05$ . We write the domain profiles on the left and  $\hat{Q}$  on the right.

$t_E^{a_0} \sim R_E \sim 1/g_E$ . This relation roughly holds in Fig. 4.

Figure 5 illustrates  $\hat{Q}$  in a pinned state at  $t = 45\,000$  for  $\phi_s = 50\%$ . It is defined by (6) and represents the degree of anisotropic deformations. We find  $\hat{Q} \cong 0$  within the harder domains in late stages ( $t \gtrsim 10^3$ ), which means that the harder domains are nearly isotropically deformed. In particular, at  $\phi_s = 70\%$  in Fig. 1, shapes of harder domains are considerably deformed from circles. Note that domain shapes are much closer to circles for  $g_E = 0$ . The harder domains deform to cancel elastic fields produced by other harder domains and to become elastically isotropic. Figure 6 illustrates such shape adjustment in a simple case of two harder domains. We prepare two circles at  $t = 0$  in a nearly saturated matrix. At  $t = 10^3$ , the interfaces facing to each other have been flattened to achieve  $\hat{Q} \cong 0$  inside and the softer region between them has been uniaxially deformed. In Figs. 1–3, we observe the same elastic deformations throughout the system.

Thus, interfaces separate uniaxially deformed softer regions and isotropic harder regions in late stages, where surface protuberances with spatial scales greater than  $R_E$  are suppressed by the elastic-free-energy cost.<sup>11</sup> Our results of  $\phi_s = 50$  and  $30\%$  suggest that two-phase structures in the presence of modulus inhomogeneity can be driven into metastable glassy states after the asymmetric elastic deformations. At  $\phi_s = 70\%$ , however, pinning does not take place in the simulation time ( $t \lesssim 4 \times 10^4$ ).

In real alloys with relatively large lattice misfits, close-

ly aligned cuboids with very slow coarsening rates are often observed and the sizes of the cuboids become uniform after a long aging time.<sup>3</sup> By further adding the cubic interaction to (8),<sup>4</sup> we can reproduce very similar frozen structures for relatively small  $\phi_s$ . Such aspects will be reported shortly elsewhere. Thus, the three long-range interactions mentioned at the beginning of this paper can, together, well explain essential morphologies observed in two-phase cubic alloys.

Finally, we should comment on Eshelby's interaction<sup>10</sup> due to  $\Delta\mu$  ( $=\mu_1\Delta c$  in our notation). He supposed two precipitates,  $A$  and  $B$ , whose shear modulus is slightly different from that of the matrix by  $\Delta\mu$ . Then the elastic energy is changed by the following amount:

$$\Delta E = \Delta\mu \int_{V_A + V_B} d\mathbf{r} \sum_{i,j} [e_{ij}^A + e_{ij}^B - \frac{1}{3}(e^A + e^B)\delta_{ij}]^2, \quad (9)$$

where the integral is within  $A$  and  $B$ ,  $e_{ij}^A$  (or  $e_{ij}^B$ ) are strains  $\frac{1}{2}(\nabla_i u_j + \nabla_j u_i)$  produced by  $A$  (or  $B$ ) only, and  $e = \nabla \cdot \mathbf{u} = \sum_i e_{ii}$ . The same contribution also follows from (5). Eshelby calculated  $\Delta E$  when  $A$  and  $B$  are both spheres. However, Fig. 6 indicates that the shear strains can vanish after shape changes and then  $\Delta E = 0$ . Within  $A$ , this means

$$e_{ij}^A - \frac{1}{3}e^A\delta_{ij} = -(e_{ij}^B - \frac{1}{3}e^B\delta_{ij}). \quad (10)$$

For large separation of  $A$  and  $B$ , the right-hand side is nearly a constant, symmetric, traceless tensor within  $A$  and, hence, (10) is indeed satisfied for an ellipsoidal shape<sup>12</sup> of  $A$ . Eshelby's interaction thus exists strictly among spheres and disappears after such shape adjustment. We must take into account shape changes even in phase separation at very small volume fractions  $\phi_h = 1 - \phi_s$  of the harder component. The elastic effect at small  $\phi_h$  still remains to be explored.<sup>13</sup> It is expected that shape changes are much more drastic for small  $\phi_s$  of the softer component.<sup>11</sup>

We acknowledge valuable discussions with Professor K. Kawasaki, Professor T. Miyazaki, and Professor M. Doi.

<sup>1</sup>A. G. Khachaturyan, *Theory of Structural Transformations in Solids* (Wiley, New York, 1983).

<sup>2</sup>R. W. Carpenter, *Acta Metall.* **15**, 1567 (1967).

<sup>3</sup>T. Miyazaki and M. Doi, *Mater. Sci. Eng. A* **110**, 175 (1989); T. Miyazaki, M. Doi, and T. Kozakai, *Solid State Phenom.* **384**, 227 (1988).

<sup>4</sup>A. Onuki, *J. Phys. Soc. Jpn.* **58**, 3065 (1989); **58**, 3069 (1989); in *Formation, Dynamics and Statistics of Patterns*, edited by K. Kawasaki, M. Suzuki, and A. Onuki (World Scientific, Singapore, 1990).

<sup>5</sup>T. Miyazaki and M. Doi (private communication). They checked the coherency for the data in Ref. 3. However, in very late stages (which were not discussed in Ref. 3), alloys often became incoherent. Then domains started to grow, roughly obeying  $a \sim \frac{1}{3}$ .

<sup>6</sup>H. Nishimori and A. Onuki, *Phys. Rev. B* **42**, 980 (1990).

<sup>7</sup>Y. Oono and S. Puri, *Phys. Rev. A* **38**, 434 (1988).

<sup>8</sup>J. W. Cahn, *Acta Metall.* **9**, 795 (1961).

<sup>9</sup>W. C. Johnson and J. W. Cahn, *Acta Metall.* **32**, 1925 (1984).

<sup>10</sup>A. J. Ardell, R. B. Nicholson, and J. D. Eshelby, *Acta Metall.* **14**, 1295 (1966).

<sup>11</sup>On the contrary, interfaces are destabilized when they separate an isotropic softer region and an anisotropically deformed harder region. This situation occurs when softer precipitates grow in a harder matrix (Refs. 4 and 9).

<sup>12</sup>J. D. Eshelby, *Proc. R. Soc. London, Ser. A* **241**, 376 (1957). He showed that the elastic strains inside ellipsoidal inclusions are homogeneous.

<sup>13</sup>K. Kawasaki and Y. Enomoto, *Physica A* **150**, 463 (1988). They showed that Eshelby's interaction becomes crucial among spheres when the average radius exceeds  $R_E/\phi$ ,  $\phi$  being the volume fraction.